Supplementary Methods

cDNA library constructions for small RNAs and mRNAs

Total RNA was extracted using the TRIzol reagent (Thermo Fisher) and chloroform, and the concentration was determined by NanoDrop (Thermo Fisher). For small RNA libraries, 20~50 μg total RNA was analysed on a 15% TBE-Urea gel, and the 18~29 nt band was excised (the ~30 nt 2S rRNA band was avoided with caution). The resolved RNAs were sequentially ligated with 3'-adaptor and 5'-adaptor, and then reverse-transcribed. See Supplementary Table S1 for the sequences of the adaptors. For mRNA libraries, 10~20 μg poly(A)+ RNAs were selected on oligo-dT25 DynaBeads (Thermo Fisher) and fragmented at 95°C in fragmentation buffer (2 mM EDTA, 12 mM Na_2CO_3, 88 mM $NaHCO_3$, pH 9.3). The fragmented RNAs within 40~80 nt were 3'-dephosphorylated, ligated with 3'-adaptor and purified on a 15% TBE-Urea gel. The 3'-ligated RNAs were subsequently 5'-phosphorylated, ligated with 5'-adaptor, and reverse-transcribed. All cDNAs were amplified through 12 PCR cycles, and the products within the correct size ranges were collected from 20% TBE gels for quality tests (Fragment Analyzer, Agilent Technologies) and sequencing (Illumina HiSeq-2500 sequencer; run type: single-end; read length: 50 nt).

Ribosome profiling of S2 cells

The harvested S2 cells were treated with 100 μg/mL cycloheximide (CHX, from Sigma) for 5 min to stop translation, washed using ice-cold PBS containing 100 μg/mL CHX, and then lysed in a buffer containing 50 mM Tris, pH 7.5, 150 mM NaCl, 5 mM $MgCl_2$, 1% Triton X-100, 2 mM DTT, 20 U/mL SuperaseIn (Thermo Fisher), 0.5 tablet of Protease inhibitor (Roche), 100 μg/mL CHX, and 100 μg/mL emetine (Sigma). The clarified lysates were aliquoted, flash-frozen in liquid nitrogen, and stored at -80°C for future RNA extraction procedures or ribosome footprinting. It has been reported that pre-treating with CHX has an impact on the ribosome footprint profiles after the start codon (1,2). To control this, all our analyses were based on the contrast between the experimental measurements and a side-by-side control measurement.

Lysates with ~400 μg total RNA were treated with micrococcal nuclease (3 U/μg RNA) in a buffer containing 50 mM Tris, pH 7.5, 15 mM $CaCl_2$, 5 mM $MgCl_2$, 1% Triton x-100, 2 mM DTT, 20 U/mL SuperaseIn, 0.5 tablet of protease inhibitor, 100 μg/mL CHX, and 100 μg/mL emetine for 40 min at 25°C. The reaction was quenched by adding EGTA to a final concentration of 6.25 mM. A 10~50% sucrose gradient was prepared in a buffer containing 250 mM NaCl, 50 mM Tris, pH 7.5, 15 mM $MgCl_2$, 0.5 mM DTT, 12 U/mL RNaseOUT, 0.5 tablet of protease inhibitor and 20 μg/mL emetine using a Gradient Master (Biocomp Instruments) and resolved using a SW-41 rotor (Beckmann Coulter). The monosome fractions were collected, flash-frozen in liquid nitrogen, and stored at -80°C until further use.

SuperaseIn was applied throughout the protocol. The resuspended monosomes were digested with 20 mg/mL Proteinase K and 10% SDS at 42°C and were subsequently extracted once using acid phenol and once using phenol/chloroform. The 28~32 nt RNA fragment band was isolated from 15% TBE-Urea gels. To remove the rRNA-derived fragments, the RNAs were treated with Ribo-Zero Gold rRNA Removal Kit (Illumina). The remaining RNAs were sequentially subject to 3'-dephosphorylation, 3'-ligation, 5'-phosphorylation, 5'-ligation, and reverse-transcription. The cDNAs were treated with synthesized biotinylated oligos (Supplementary Table S1) on DynaBeads for further depletion of the rRNA-derived products and were subjected to the same procedures described above.

Sequence processing and alignment

The FASTX-Toolkit (http://hannonlab.cshl.edu/fastx_toolkit/) was applied to clip the 3'-adaptor sequence from reads that had passed purity filtering. After clipping, small RNA-Seq reads within 18~29 nt, mRNA-Seq reads more than 40 nt and Ribo-Seq reads within 27~35 nt were kept. The remaining reads were sequentially mapped to the yeast genome (S288C_R64.2.1), the *Wolbachia* genome (GenBank), 23 species of insect virus (GenBank), transposons (FlyBase), miscRNA (FlyBase), miRNAs (miRBase) and tRNAs (3), using Bowtie version 1.0.1 (4). The unmapped reads were subsequently aligned with

chromosome arms (FlyBase r6.06) using STAR (5). Antisense (less than 0.1%) and non-unique alignments (less than 1%) for the protein-coding genes were discarded in further quantitative analyses. See Supplementary Table S4 for the summary of the mapping statistics.

Quantifications of small RNA, mRNA and RPF expression

For each the protein-coding gene, the transcript isoform with the longest CDS was used to represent the expression level. The mRNA-Seq reads that were mapped to the exons of these transcripts, and the Ribo-Seq reads that were mapped to the CDSes of these transcripts, were summarized with HTSeq-count (6). For the differential expression analysis, the count data were normalized and analysed using DESeq2 (7), while genes with extremely low expression (< 50 summed reads in all replicates and experiments for each library preparation procedure) were excluded. Significantly regulated genes were considered when $|\log_2$ fold change$| > 0.2$ and FDR adjusted P-value < 0.05. The functional annotation of the significantly regulated genes was obtained using DAVID (http://david.ncifcrf.gov).

Supplementary References

1. Gerashchenko, M.V. and Gladyshev, V.N. (2014) Translation inhibitors cause abnormalities in ribosome profiling experiments. *Nucleic Acids Res.*, **42**, e134.
2. Hussmann, J.A., Patchett, S., Johnson, A., Sawyer, S. and Press, W.H. (2015) Understanding biases in ribosome profiling experiments reveals signatures of translation dynamics in yeast. *PLoS Genet.*, **11**, e1005732.
3. Lowe, T.M. and Eddy, S.R. (1997) tRNAscan-SE: a program for improved detection of transfer RNA genes in genomic sequence. *Nucleic Acids Res.*, **25**, 955-964.
4. Langmead, B., Trapnell, C., Pop, M. and Salzberg, S.L. (2009) Ultrafast and memory-efficient alignment of short DNA sequences to the human genome. *Genome Biol.*, **10**, R25.
5. Dobin, A., Davis, C.A., Schlesinger, F., Drenkow, J., Zaleski, C., Jha, S., Batut, P., Chaisson, M. and Gingeras, T.R. (2013) STAR: ultrafast universal RNA-seq aligner. *Bioinformatics*, **29**, 15-21.
6. Anders, S., Pyl, P.T. and Huber, W. (2015) HTSeq--a Python framework to work with high-throughput sequencing data. *Bioinformatics*, **31**, 166-169.
7. Love, M.I., Huber, W. and Anders, S. (2014) Moderated estimation of fold change and dispersion for RNA-seq data with DESeq2. *Genome Biol.*, **15**, 550.

Supplementary Figures

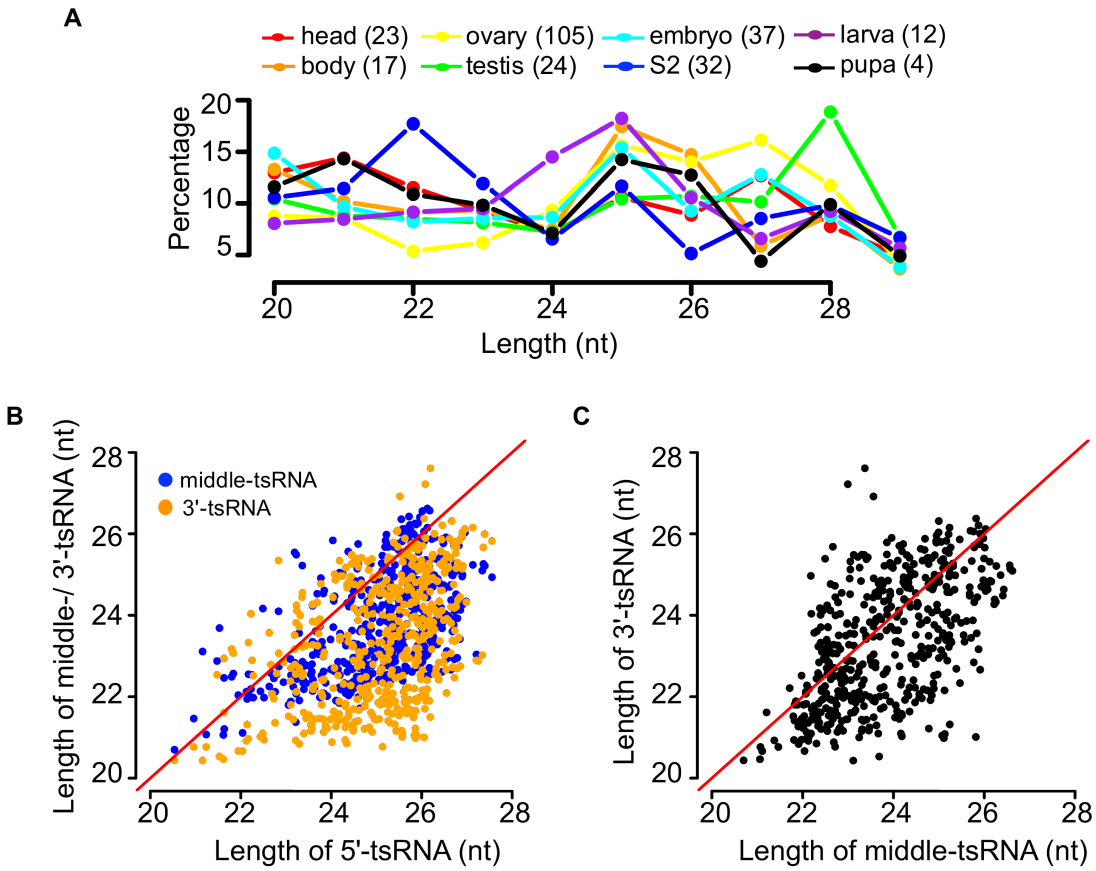

Figure S1. Length distribution of tsRNAs.
(A) The distributions of the tsRNA length in different developmental tissue/development stages. The color key represents the percentage (%) of tsRNAs with a certain length in a library. The number of libraries in each type is indicated in parentheses.
(B) The lengths of the 5'-tsRNAs are generally longer than those of the middle-tsRNAs (blue) and 3'-tsRNAs (orange) in a library.
(C) The lengths of the middle-tsRNAs are generally longer than those of the 3'-tsRNAs in a library. The libraries plotted in (B) and (C) are the 495 public libraries listed in Supplementary Table S2.

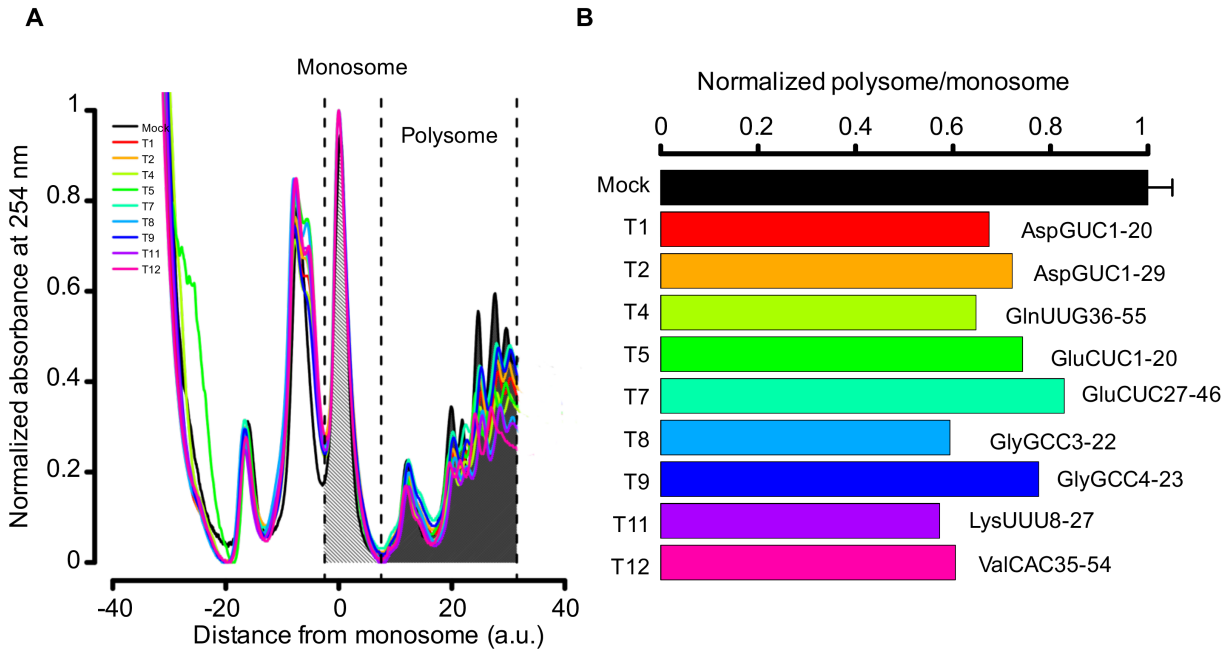

Figure S2. Transfections of tsRNA mimics into S2 cells repress global translational activities.
(A) Absorbance profiles (at a UV wavelength of 254 nm) of RNAs partitioned using 10~45% sucrose gradients from S2 cells transfected without any RNA sequence (Mock, black), with different single-stranded tsRNA mimics (T1 to T12, without the three tsRNA mimics in Figure 2B). For each profile, both the absorbance and the position were normalized according to the monosome peak. Dashed lines indicate the boundaries of the monosome and polysome partitions for a measurement of the overall translational activity. Error bars for the Mock represent one standard deviation computed from three repeated experiments.
(B) The ratios of the aggregate intensities within polysome partition (P) to the monosome partition (M) normalized by the median value of the control experiments. For each cellular transfection experiment, the ID of each tsRNA is given to the left of the plot, and the start and end positions of the tsRNA on the source tRNA were given to the right of the bar plot.

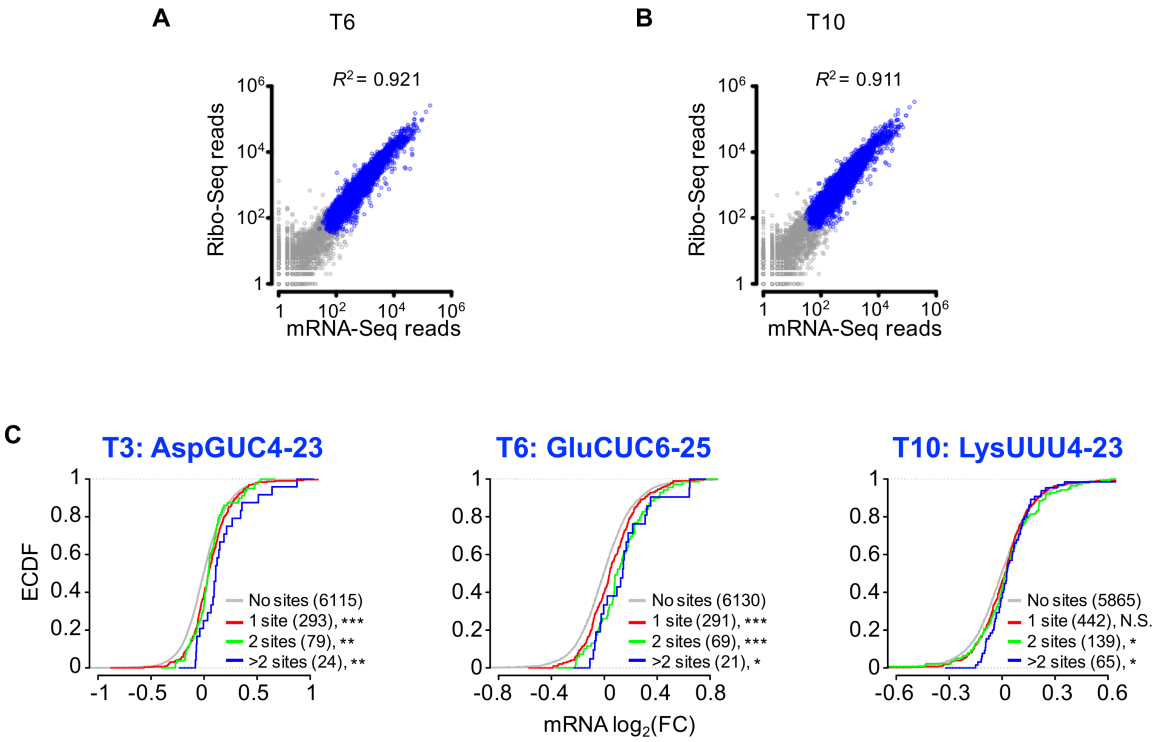

Figure S3. tsRNAs transfected into S2 cells repress mRNAs with conserved target sites.
(A-B) Scatter plots of the Ribo-Seq read counts against the mRNA-Seq read counts of individual genes in T6 (A) and T10 (B) transfection experiments. Blue circles represent genes that have > 50 mRNA-Seq reads and >50 Ribo-Seq reads.
(C) Cumulative distribution of gene expression changes in mRNA. The *x-axis* is the $\log_2(FC_{mRNA})$ of mRNA in S2 cells transfected with the tsRNA mimic (T3, T6, T10 from left to right) versus transfection with ss-NC. The genes with 7-mer sites conserved between *D. melanogaster* and *D. virilis* and antisense paired to any part of a tsRNA are defined as tsRNA target genes. Red: genes with one conserved tsRNA target site, Green: genes with two conserved tsRNA target sites, Blue: genes with more than two conserved tsRNA target sites, Grey: genes without any target site of the transfected tsRNA in the entire mRNA. The number of genes in each category is indicated in parentheses. The asterisks indicate a significant difference in mRNA fold change compared with the ss-NC control group. *, $P < 0.05$; **, $P < 0.01$; ***, $P < 0.001$, N.S. not significant.

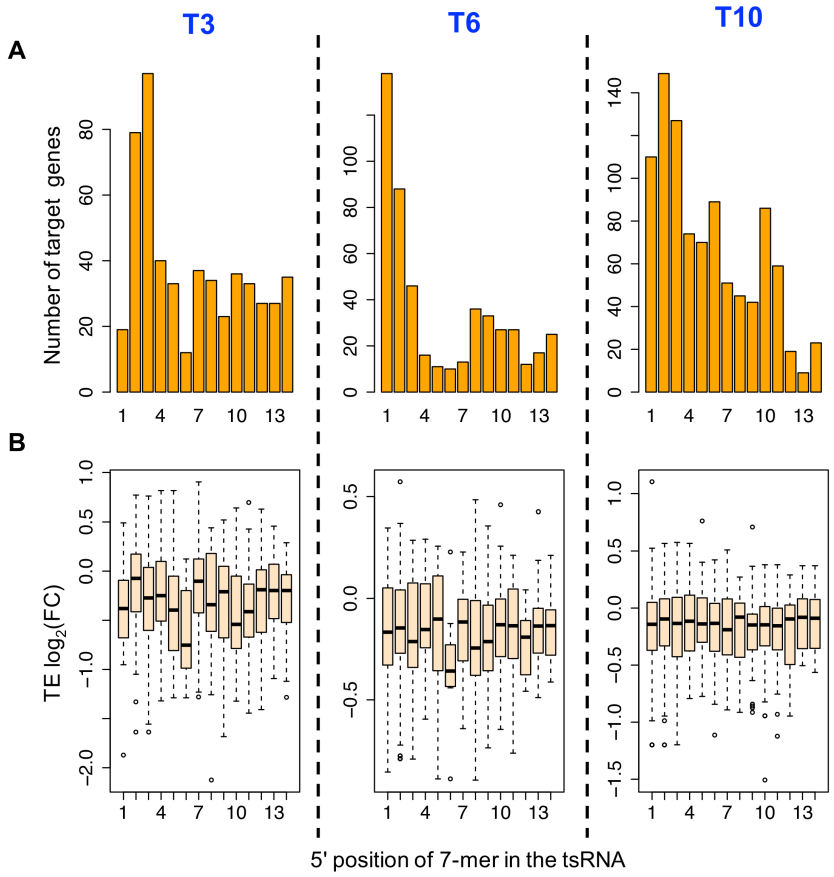

Figure S4. tsRNAs transfected into S2 cells repress mRNAs with conserved target sites.
(A) The number of conserved 7-mer target sites antisense pairing to different regions of a tsRNA. For each target site, the starting position of pairing in the tsRNA was shown. From left to right, T3, T6, and T10.
(B) Changes of TEs for target genes with complementary sites of 7-mers starting from different positions of tsRNA. From left to right, T3, T6, T10 transfection.

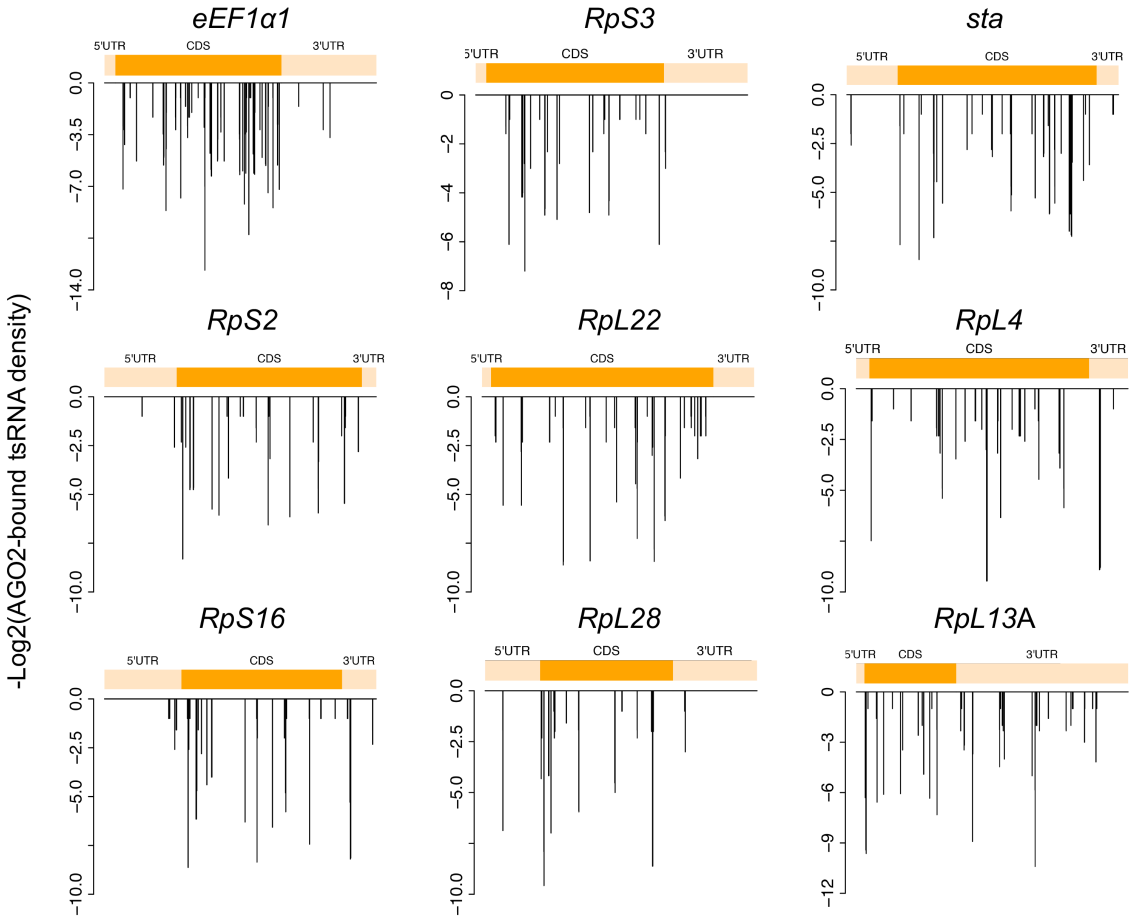

Figure S5. The density of conserved target sites of the AGO2-bound tsRNAs on representative mRNAs. The *y-axis* is the -$\log_2$ (reads of AGO2-bound tsRNAs) for each target site.

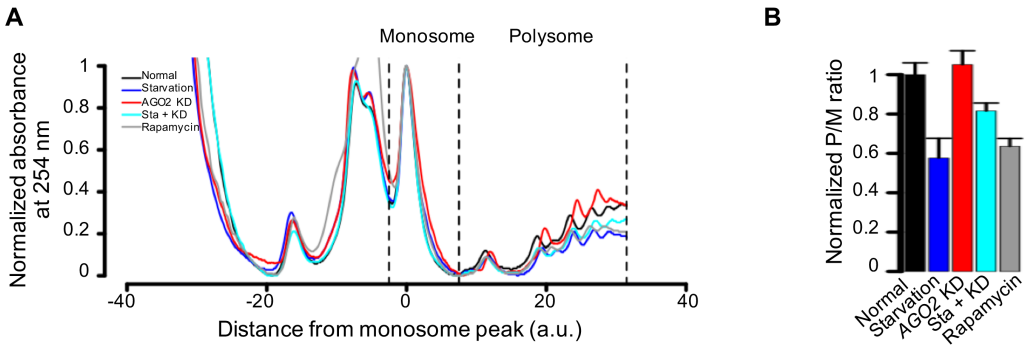

Figure S6. The polysome profile analysis for RNAs in S2 cells under different conditions.
(A) The polysome profiles for RNAs in S2 cells under the conditions of normal culture (black), serum starvation (blue), *AGO2* knockdown (red), *AGO2* knockdown while serum deprived (cyan), and rapamycin treatment (grey).
(B) The relative P/M ratios measured from S2 cells under different conditions as in (A). Error bars represent one standard deviation computed from three repeated experiments.

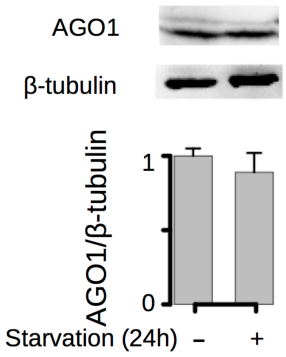

Figure S7. Level of AGO1 remains similar after starvation in S2 cells. Western blotting shows no significant difference in the level of AGO1 proteins after 24 hours culturing in the serum-free medium. Error bars represent one standard deviation computed from two repeated experiments.

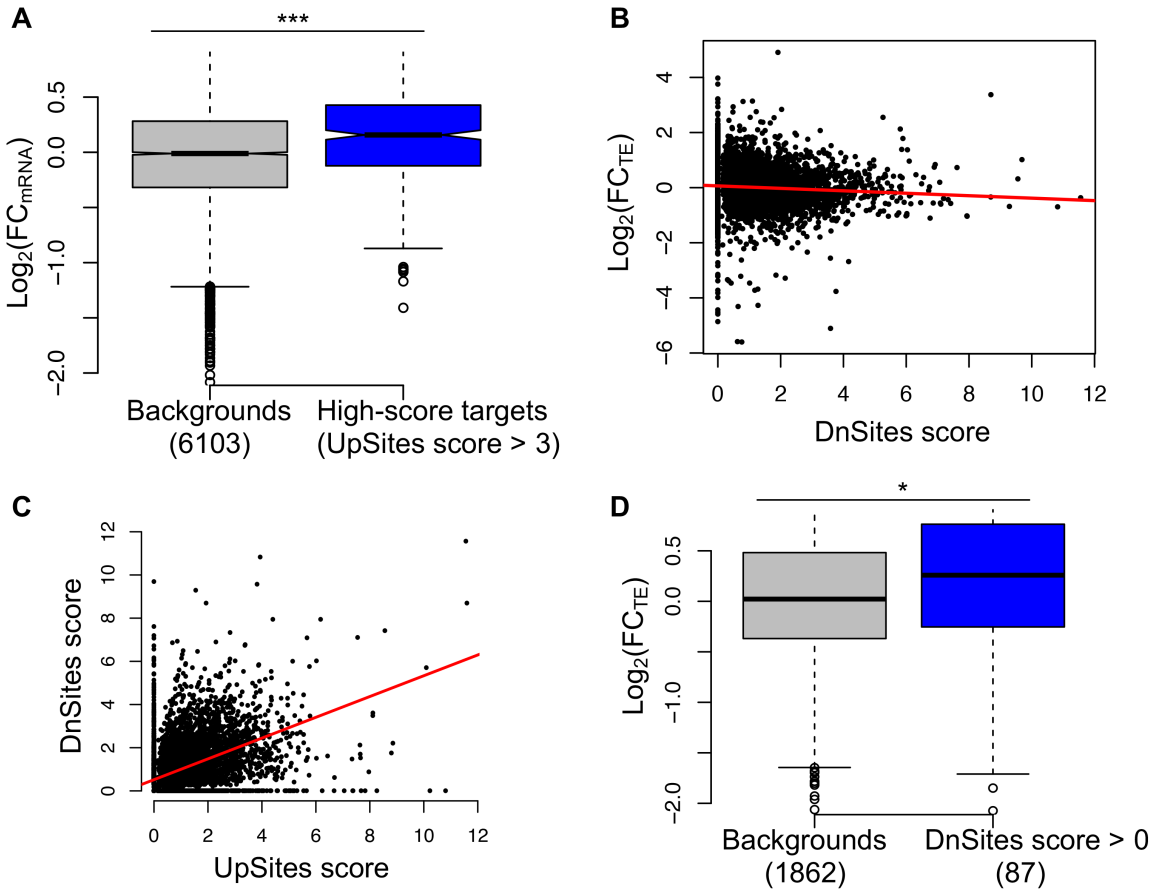

Figure S8. Changes of mRNA levels and TEs for genes targeted by the up-regulated or down-regulated tsRNAs under cellular starvation.

(A) The mRNAs of the highest scoring target genes (UpSites score > 3) were significantly up-regulated compared to those of the background genes in the starved S2 cells. ***, $P < 0.001$.

(B) A significantly negative correlation between the FC_{TE} (log_2 scaled, *y-axis*) and the DnSites score for a mRNA under starvation ($\varrho = -0.075$, $P = 1.2\times10^{-9}$).

(C) The UpSites and DnSites scores for a mRNA were highly correlated ($\varrho = 0.478$, $P < 10^{-16}$).

(D) Among the mRNAs without any sites of the up-regulated tsRNAs (UpSites = 0), the target mRNAs of the down-regulated tsRNAs had significantly higher TEs compared to the remaining mRNAs. *, $P < 0.05$.

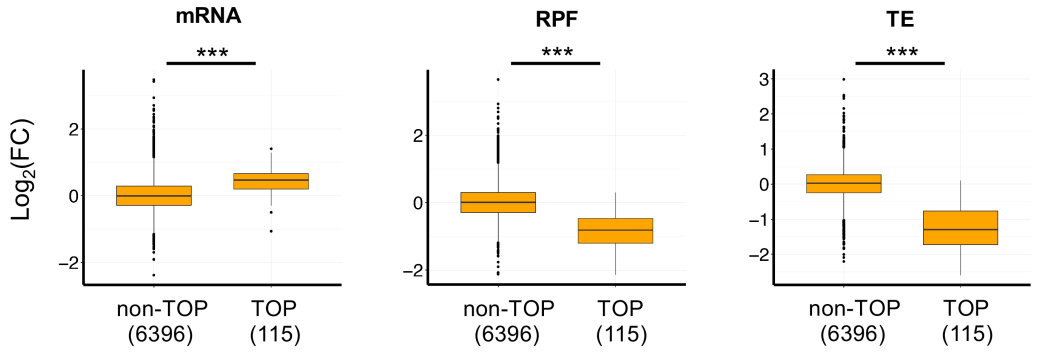

Figure S9. The $\log_2$(FC) of mRNA, RPF and TE after rapamycin treatment in S2 cells. The number of genes in each category is indicated in parentheses. ***, $P < 0.001$.

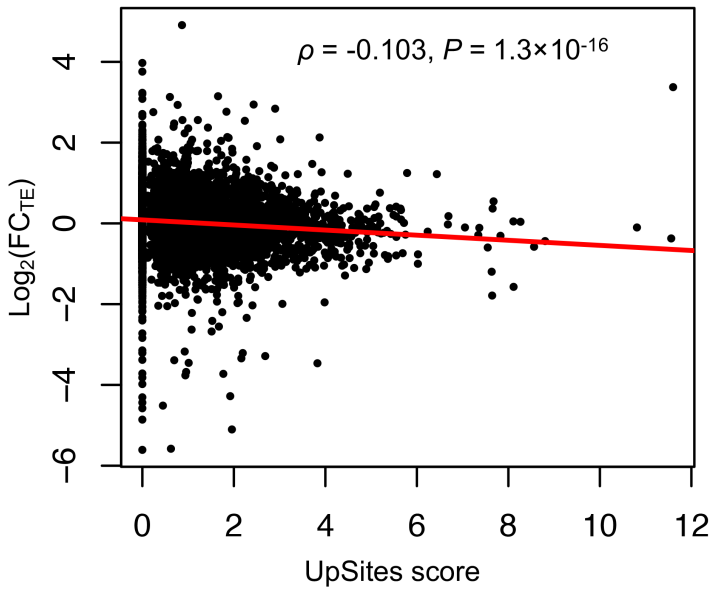

Figure S10. A significantly negative correlation between FC_{TE} ($\log_2$ scaled) and the UpSites score for a mRNA under starvation (the 5'TOP genes were removed).

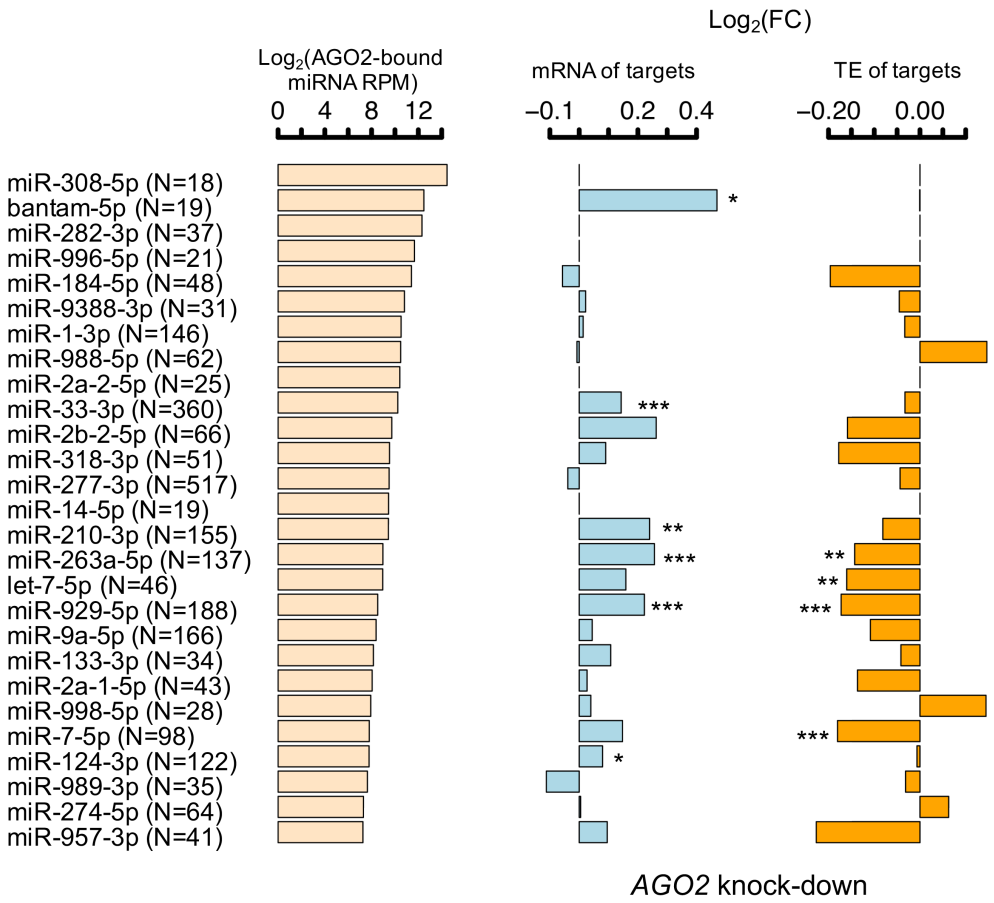

Figure S11. The change of expression for target genes of the AGO2-bound miRNAs in *AGO2* knock-down S2 cells. The AGO2-bound miRNAs are preferentially bound with AGO2 rather than AGO1 in IP-Seq experiments. The number of target genes in each miRNA is indicated in parentheses. *, $P < 0.05$; **, $P < 0.01$; ***, $P < 0.001$.

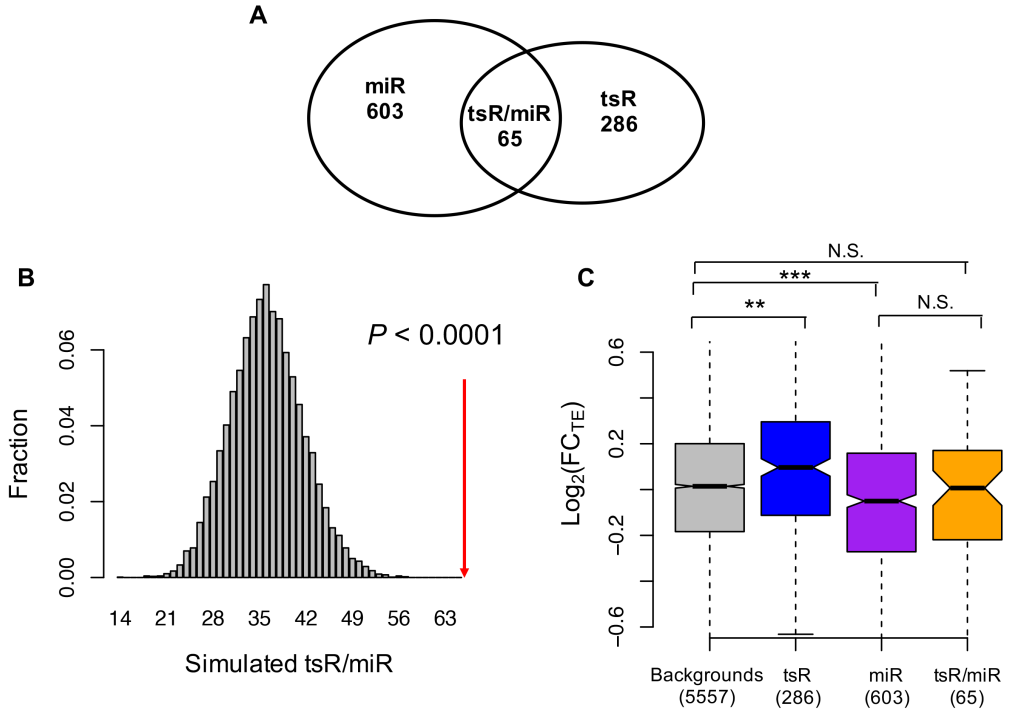

Figure S12. The overlapping of target genes of the tsRNAs and AGO2-bound miRNAs in normal S2 cells.

(A) The overlap between targets of AGO2-bound tsRNA and targets of AGO2-bound miRNA. tsR: mRNAs with conserved target sites of AGO2-bound tsRNAs with the density > 1.5 per kb of mRNA; "miR": the conserved canonical target sites of the AGO2-bound miRNAs in S2 cells.

(B) The observed number of mRNAs that were targeted by the miRNAs and tsRNAs (65, red) and the simulated number of target mRNAs shared between miRNAs and tsRNAs (*x-axis*). In each round of simulation, the observed numbers of miRNA targets and tsRNA targets were randomly sampled from the genes expressed in S2 cells (6,511 genes) respectively, and then the number of targets overlapped between the two sets were counted. The simulation was replicated for 10,000 replicates.

(C) The $\log_2$(FC) of TE (*y-axis*) for genes in the *AGO2* knock-down S2 cells. "tsR" represents mRNAs only with strong target sites of AGO2-bound tsRNAs; "miR" represents mRNAs only with AGO2-bound miRNAs target sites; "tsR/miR" represents genes with both strong target sites of AGO2-bound tsRNA and target sites of AGO2-bound miRNAs; "backgrounds" means the remaining genes expressed in S2 cells. The number of genes in each category is indicated in parentheses. **, $P < 0.01$; ***, $P < 0.001$; N.S. not significant.

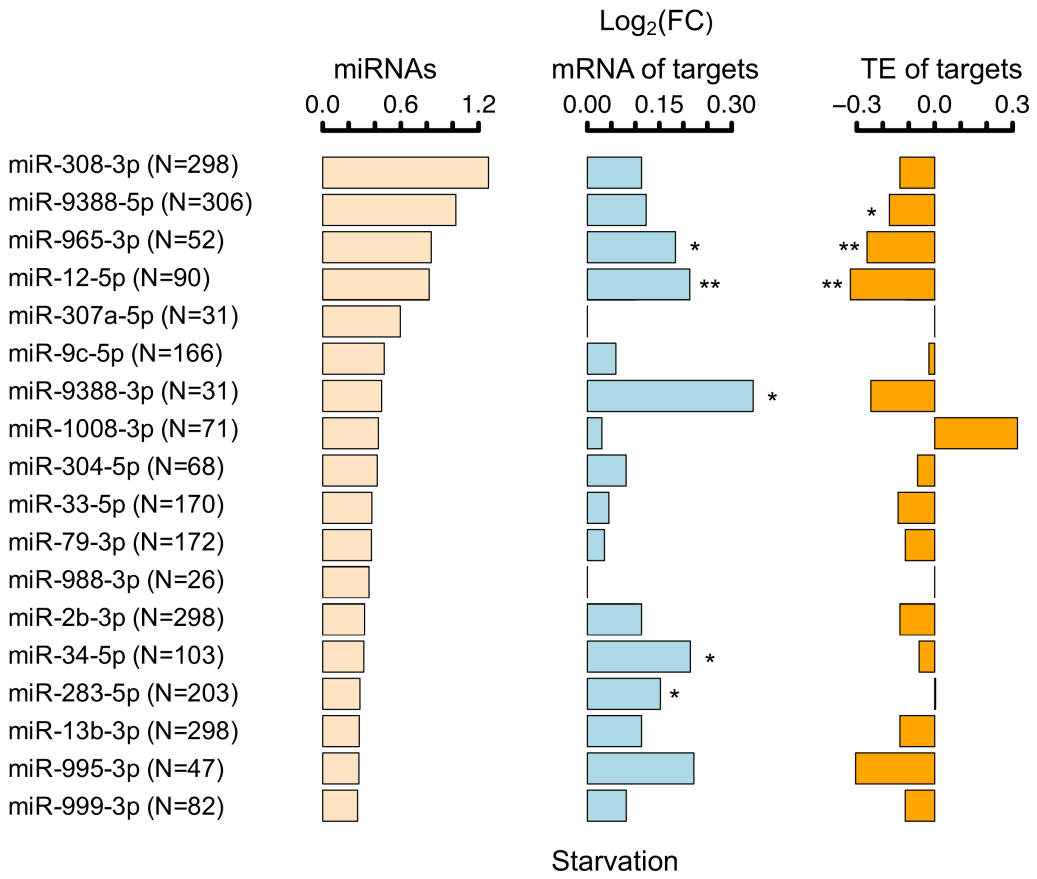

Figure S13. The miRNAs up-regulated in the starved relative to the normal S2 cells, and the $\log_2$(FC) for mRNAs and TEs of the conserved target genes. The 18 up-regulated miRNAs have expression change > 1.2 folds in the starved S2 cells. The number of conserved target genes in each miRNA is indicated in parentheses. *, $P < 0.05$, **, $P < 0.01$.

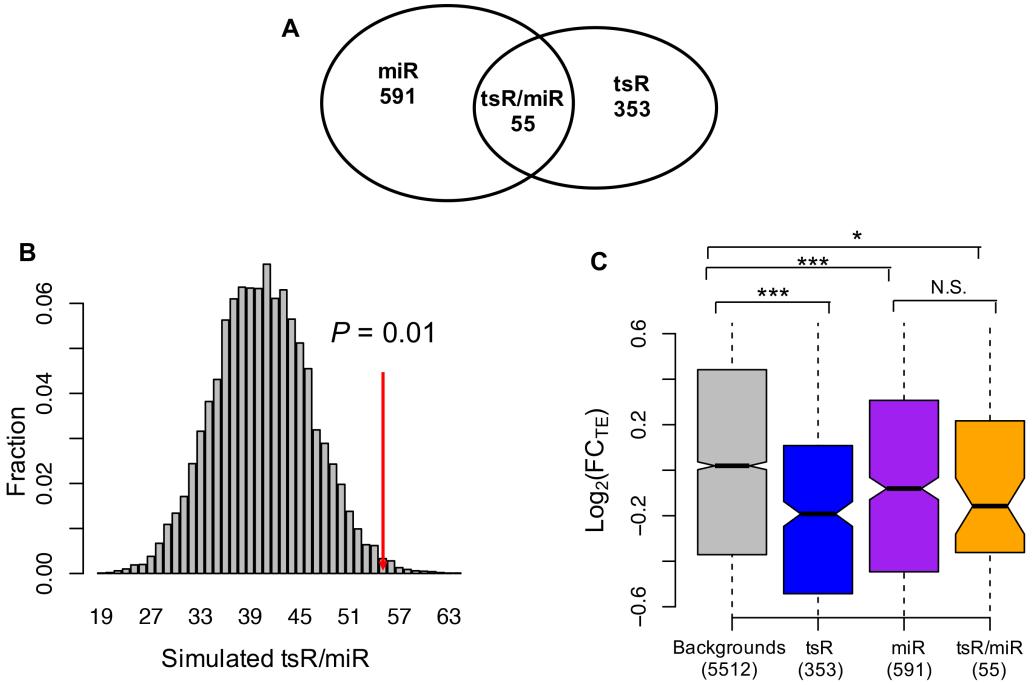

Figure S14. The overlapping of target genes of the up-regulated tsRNAs and AGO2-bound miRNAs in the starved S2 cells.

(A) The overlap between targets of AGO2-bound tsRNA and targets of AGO2-bound miRNAs that were up-regulated under starvation. tsR: mRNAs of the up-regulated tsRNAs with UpSites score > 3 but not targeted by the up-regulated miRNAs; "miR": the conserved canonical target sites of the AGO2-bound miRNAs in S2 cells that were not targeted by the up-regulated tsRNAs. tsR/miR: mRNAs targeted by both the up-regulated tsRNAs and miRNAs.

(B) The observed number of mRNAs that were targeted by the up-regulated miRNAs and tsRNAs (55, red) and the simulated number of target mRNAs shared between the up-regulated miRNAs and tsRNAs (*x-axis*). In each round of simulation, the observed numbers of miRNA targets and tsRNA targets were randomly sampled from the genes expressed in S2 cells (6,511 genes) respectively, and then the number of targets overlapped between the two sets were counted. The simulation was replicated for 10,000 replicates.

(C) The $\log_2$(FC) of TE (*y-axis*) for genes in the *AGO2* knock-down S2 cells. "backgrounds" means the remaining genes expressed in S2 cells after excluding the tsR, miR and tsR/miR. The number of genes in each category is indicated in parentheses. *, $P < 0.05$; ***, $P < 0.001$; N.S. not significant.

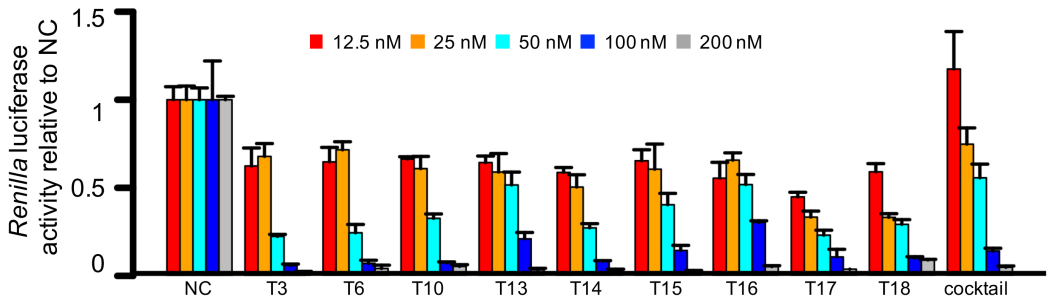

Figure S15. Co-transfection of tsRNA mimics and the psiCHECK-2 plasmids into S2 cells reduced the activities of *Renilla* luciferase. The color key shows different final concentrations of tsRNA mimics. The tsRNA cocktail was made by mixing equal amount of the nine tsRNA mimics of the same concentrations. The luciferase activity of S2 cells transfected with the tsRNA mimics were normalized by those transfected with ss-NC at the same concentration (three replicates were performed for each assay).

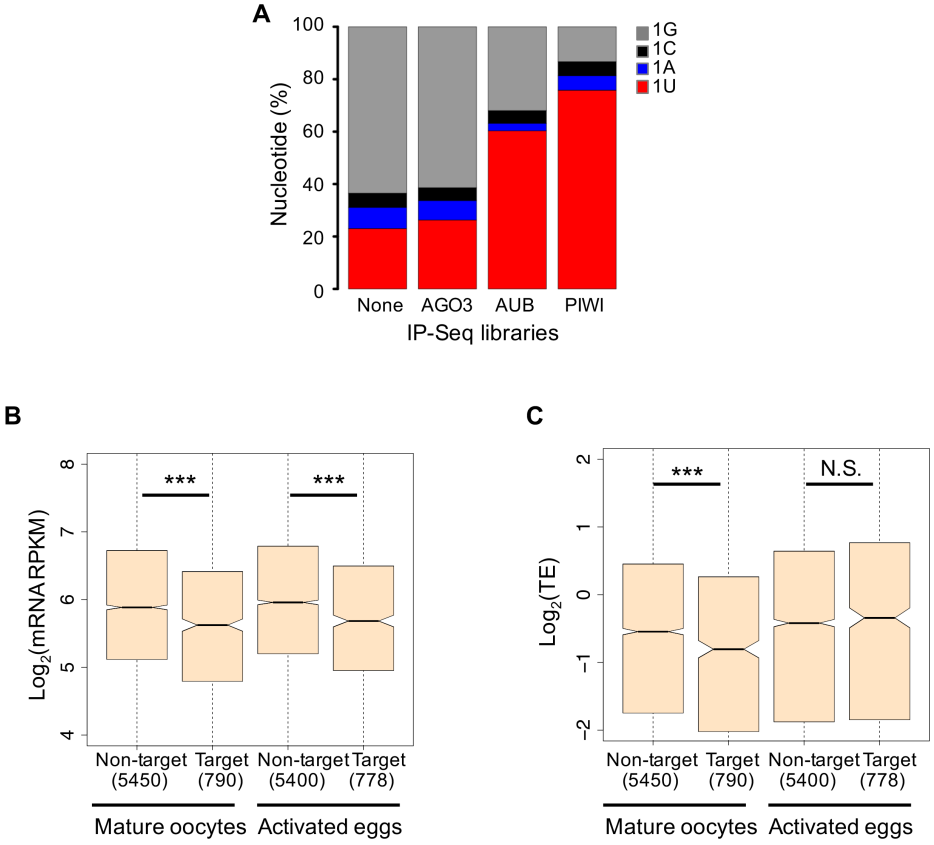

Figure S16. Predicted targets of the long tsRNAs have reduced mRNA and TEs in mature oocytes and activated eggs.

(A) Composition of the first nucleotide in tsRNAs that were detected in wildtype and not-treated libraries (None, N = 51), AGO3 (N = 12), AUB (N = 13) and PIWI-IP libraries (N = 31) of the *Drosophila melanogaster* ovaries.

(B-C) The $\log_2$ mRNA RPKM and TE of non-target genes and target genes of long tsRNAs. RNAhybrid was used to search for target sites that were complementary to the nucleotides 2-11 of the AUB-bound tsRNAs. The mRNA and Ribo-Seq datasets of mature oocytes and activated eggs were taken from I. Kronja, *et. al*. 2014 to calculate TE for each gene. The number of genes in each category is indicated in parentheses. *, $P < 0.05$, **, $P < 0.01$, ***, $P < 0.001$

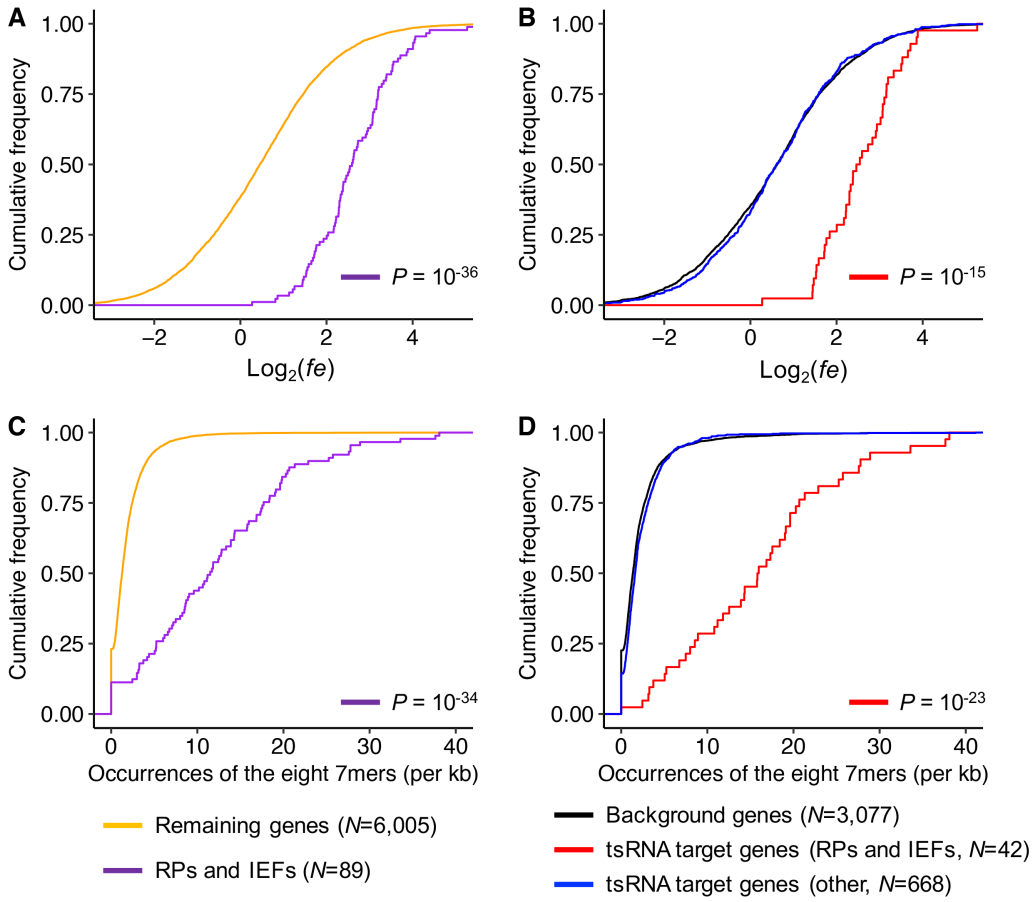

Figure S17. The fold enrichment (*fe*) of mRNAs of RPs/IEFs in AGO2 CLIP-Seq of nuclear extracts from *Drosophila* S2 cells.

(A) RPs/IEFs (purple) have significantly higher $\log_2(fe)$ scores than the remaining expressed genes (RPKM ≥ 1, orange). A higher *fe* score means the mRNA is more enriched in the AGO2 CLIP-Seq data.

(B) The cumulative frequency of $\log_2(fe)$ scores for the target genes of tsRNAs (the density of tsRNA target site > 1 per kb of mRNA) and background genes (the density of tsRNA target sites < 0.5 per kb of mRNA). Among the target genes, RPs/IEFs (N = 42, red) have significantly higher *fe* scores than the background genes.

(C) RPs/IEFs (purple) have significantly higher densities of the eight 7-mer motifs than the remaining expressed genes (RPKM ≥ 1, orange). In a gene, the occurrences of each of the eight motifs in CDS are summed and then normalized by the length of the CDS.

(D) The cumulative frequency of the occurrences of the eight 7-mers per kb for gene categories shown in (B).

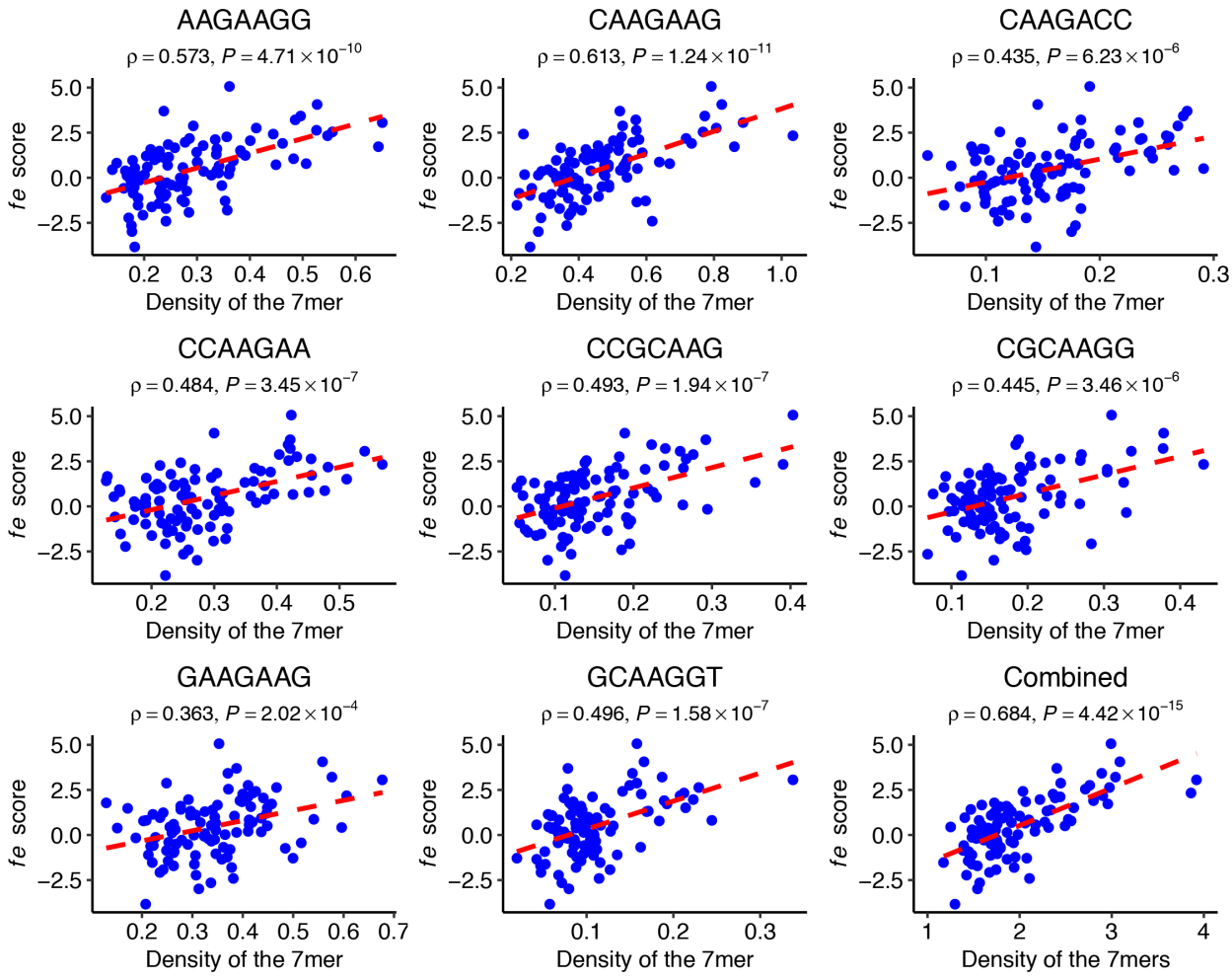

Figure S18. The density of the 7-mer motifs in the CDS regions (per kb, *x*-axis) is significantly positively correlated with the *fe* scores (*y*-axis, $\log_2$ scaled) of the mRNAs in the AGO2 CLIP-Seq data. The genes were grouped into 100 bins based on increasing densities of the 7-mer motif. In each bin, the mean *fe* score is calculated and used in the correlation analysis. Combined: the occurrences of the eight 7-mer motifs in a CDS were summed and normalized by the length of the CDS.

Supplementary Tables

Table S1. Oligomer sequences in this study

ID	Oligo sequence (5'-3')
Negative control (NC)	
Single-stranded	UUCUCCGAACGUGUCACGUUU
Double-stranded	
guide strand	UUCUCCGAACGUGUCACGUUU
passenger strand	ACGUGACACGUUCGGAGAAUU
Adaptors used for library generation	
3' adaptor	TGGAATTCTCGGGTGCCAAGG
5' adaptor	GUUCAGAGUUCUACAGUCCGACGAUC
Oligos for removal of rRNA	
Dro-01	ATGTATGTAAGCGTATTACCGGTGG
Dro-02	GCTTGGACTACATATGGTTGAGGGTTGTA
Dro-03	ATGTAAGTGGAGCCGTACCTGTTGGTTTGTCCC
Dro-04	AGTTACGTAGCCAATTGTGGAACTTTCTTGCT
Dro-05	CATTGTAATCTATTAGCATATACCAAATTT
Dro-06	TGATAAAGTGCTGATAGATTTATATGATTA
Dro-07	GCTAATTAACACAATCCCGGCGTTCTAT
Dro-08	ACGACAATGGATGTGATGCCAATGTAATTT
Dro-09	GGTTGAACTCTAGATAACATGCAGATCGTA
Dro-10	TTTGATGCAAGCTTCTTGATCAAAGTATCACGAGT
Dro-11	TGCATTGTATGGCTTCTAAACCATTTAAAGTTTAT
Dro-12	CTTGGACTACATATGGTTGAGGGTTG
Dro-13	TTGGACTACATATGGTTGAGGG
Dro-14	ATTAGGCTAAAACCAAGCGATCGCAAGATCG
Dro-15	ACAACCTCAACTCATATGGGACTACCCCCTGA
Dro-16	ACGATGCCAGCTAGCAATTGGGTGTAGC
Dro-17	TTGCCAAAGATGTTTTCATTAATCAAGAACGA
Dro-18	ATAACTGTGGTAATTCTAGAGCTAATACAT
Dro-19	AACTCTAAGCGGTGGATCACTCGGCTCATGGG
Dro-20	AGGTCGTATCCGTGCTGGACTGCAATGATAA
Dro-21	CATTGTGATGGCCCTAGCGGGTGTTGACACAA
Dro-22	TGTGCTTTTATTAGGCTAAAACCAAGCG

Table S2: A summary of the 495 publicly available deep-sequencing libraries of small RNAs. See the excel file Table S2.xlsx

Table S3. Synthetic tsRNA sequences that were used to transfect S2 cells.

ID	tsRNA	Sequence (5'-3')	total reads	AGO1-IP	AGO2-IP
T1	AspGUC1-20	UCCUCGAUAGUAUAGUGGUU	7028730	10	106
T2	AspGUC1-29	UCCUCGAUAGUAUAGUGGUUAGUAUCCCC	1962792	2	21
T3	AspGUC4-23	UCGAUAGUAUAGUGGUUAGU	348507	2	4
T4	GlnUUG36-55	GAAUCCAGCGAUCCGAGUUC	12376	13	162
T5	GluCUC1-20	UCCCAUAUUGUCUAGUGGUU	11718113	0	3
T6	GluCUC6-25	UAUUGUCUAGUGGUUAGGAU	111766	0	2
T7	GluCUC27-46	UCCGGCUCUCACCCGGGAGG	675	0	0
T8	GlyGCC3-22	AUCGGUGGUUCAGUGGUAGA	6215393	3	1
T9	GlyGCC4-23	UCGGUGGUUCAGUGGUAGAA	354123	4	8
T10	LysUUU4-23	CGGAUAGCUCAGUCGGUAGA	277609	0	2
T11	LysUUU8-27	UAGCUCAGUCGGUAGAGCAU	152529	18	1
T12	ValCAC35-54	ACACGCACAAGGUCCCCGGU	10325	1	41

Each tsRNA is denoted by the start and end positions on the mature tRNA, which is specified by the amino acid it carries and the anti-codon it utilizes. Total reads are calculated from all the public small RNA libraries of *D. melanogaster* (N = 457). Shown also are the read counts in two AGO1-IP (GSM280088 and SRR768820) and corresponding two AGO2-IP small RNA libraries of S2 cells (GSM280087 and SRR768821).

Table S4 Mapping statistics of the mRNA-Seq and Ribo-Seq experiments

type	condition	clean reads	reads mapped to genome
starvation treatment			
mRNA-seq	normal	30771296	17255091
mRNA-seq	starvation	48638217	5175823
ribo-seq	normal	33371505	21670364
ribo-seq	starvation	26395905	22490933
small RNA seq	normal	10884480	9161200
small RNA seq	starvation	11107067	9822937
AGO2 knockdown			
mRNA-seq	ds-NC transfection	32667521	22809027
mRNA-seq	*AGO2* KD	18092742	11431529
mRNA-seq	starvation + *AGO2* KD	15525179	9684257
ribo-seq	ds-NC transfection	55578816	24713009
ribo-seq	*AGO2* KD	65922080	33578587
ribo-seq	starvation + *AGO2* KD	64430727	43746247
rapamycin treatment			
mRNA-seq	DMSO	14708114	5939807
mRNA-seq	rapamycin treatment	14556550	6461919
ribo-seq	DMSO	75758596	47194822
ribo-seq	rapamycin treatment	76611149	48465584
tsRNA mimic transfection			
mRNA-seq	ss-NC transfection	17860492	8335013
mRNA-seq	T3 transfection	16597319	7213055
mRNA-seq	T6 transfection	16599633	8078531
mRNA-seq	T10 transfection	19076124	8496949
ribo-seq	ss-NC transfection	64813911	31081119
ribo-seq	T3 transfection	47873363	38767534
ribo-seq	T6 transfection	60341814	41845666
ribo-seq	T10 transfection	54744239	28539579

Table S5. Changes of the tsRNA distribution in different genetic backgrounds.

Mutant	20-22 nt	23-29 nt	Control	20-22 nt	23-29 nt	Fold Change
loqsKO/CyO	31958	183403	+/+	64858	131992	0.35
dcr-2^L811fsX	14007	75530	dcr-2^L811fsX/CyO	89719	247206	0.51
r2d2^1	37395	137360	r2d2^1/CyO	12945	26457	0.56
loqs^f00791	142539	285868	loqs^f00791/CyO	118240	182625	0.77

Libraries that were generated with additional treatments such as immunoprecipitation and oxidization, or datasets that do not have available appropriate control data from the same studies, were not used. We found a large variation in the results between different studies using the RNAi/dsRNA method, so these datasets were not used either. For each pair, the ratio of the 20-22 nt tsRNAs to the 23-29 nt tsRNAs in the mutant library was divided by this ratio in the control library to calculate the fold difference.

Table S6 5'TOP gene list

Gene ID	Gene Symbol	Ribosomal Protein	Initiation/ Elongation Factor?	Source	tsRNA Target?	Rapamycin-treatment log_2(FC)			*AGO2* knock-down log_2(FC)		
						mNRA	RPF	TE	mNRA	RPF	TE
FBgn0002607	RpL19	YES	No	Known	YES	0.65	-1.31	-1.97	0.27	0.67	0.40
FBgn0002622	RpS3	YES	No	Known	YES	0.64	-1.00	-1.64	0.04	0.72	0.68
FBgn0002626	RpL32	YES	No	Known	YES	0.57	-0.88	-1.45	0.13	0.94	0.81
FBgn0010408	RpS9	YES	No	Known	YES	0.67	-1.33	-2.00	0.32	0.80	0.48
FBgn0011284	RpS4	YES	No	Known	YES	0.40	-1.21	-1.61	0.40	1.04	0.64
FBgn0015288	RpL22	YES	No	Known	YES	0.53	-0.81	-1.34	0.86	0.67	-0.19
FBgn0017579	RpL14	YES	No	Known	YES	0.64	-1.35	-1.99	0.16	0.57	0.41
FBgn0026372	RpL23A	YES	No	Known	YES	1.07	-0.21	-1.28	0.45	0.15	-0.30
FBgn0029785	RpL35	YES	No	Known	YES	0.46	-1.18	-1.64	0.22	0.58	0.36
FBgn0031980	RpL36A	YES	No	Known	YES	0.19	-1.20	-1.39	0.33	0.97	0.63
FBgn0034743	RpS16	YES	No	Known	YES	0.77	-0.58	-1.35	0.24	0.58	0.34
FBgn0037351	RpL13A	YES	No	Known	YES	1.41	-0.76	-2.17	0.61	0.65	0.03
FBgn0038834	RpS30	YES	No	Known	YES	0.46	-1.03	-1.49	0.07	0.41	0.34
FBgn0039857	RpL6	YES	No	Known	YES	0.62	-0.82	-1.44	0.32	0.27	-0.05
FBgn0261602	RpL8	YES	No	Known	YES	1.29	-1.30	-2.59	0.50	0.68	0.18
FBgn0261608	RpL37A	YES	No	Known	YES	0.49	-0.68	-1.17	0.76	0.78	0.02
FBgn0010411	RpS18	YES	No	Known	YES	0.42	-1.13	-1.54	0.40	0.86	0.47
FBgn0020618	Rack1	No	No	Known	YES	0.68	-0.46	-1.14	0.48	0.95	0.47
FBgn0000556	Ef1alpha48D	No	YES	Known	YES	0.47	-1.72	-2.19	0.41	0.76	0.35
FBgn0000559	EF2	No	YES	Known	YES	0.01	-0.75	-0.76	0.10	0.68	0.59
FBgn0022023	eIF-3p40	No	YES	Known	YES	0.50	-0.46	-0.96	0.19	0.82	0.63
FBgn0025582	Int6	No	YES	Known	YES	0.04	-0.80	-0.84	0.27	0.54	0.27
FBgn0003941	RpL40	YES	No	Novel	YES	0.12	-0.82	-0.94	0.23	0.52	0.30
FBgn0003942	RpS27A	YES	No	Novel	YES	0.20	-1.76	-1.96	0.44	0.92	0.49
FBgn0005533	RpS17	YES	No	Novel	YES	0.41	-1.91	-2.31	0.40	1.17	0.77
FBgn0010265	RpS13	YES	No	Novel	YES	0.22	-0.48	-0.69	0.13	0.47	0.34
FBgn0016726	RpL29	YES	No	Novel	YES	0.17	-1.67	-1.84	0.27	1.42	1.15
FBgn0035422	RpL28	YES	No	Novel	YES	0.63	-1.20	-1.82	0.35	1.10	0.76
FBgn0039757	RpS7	YES	No	Novel	YES	0.63	-0.52	-1.14	-0.04	0.68	0.72
FBgn0261596	RpS24	YES	No	Novel	YES	0.61	-1.28	-1.89	0.06	0.63	0.57
FBgn0000116	Argk	No	No	Novel	YES	-0.14	-0.70	-0.56	-0.38	-0.43	-0.05
FBgn0039830	ATPsynC	No	No	Novel	YES	-0.13	-0.72	-0.59	-0.01	0.28	0.28
FBgn0010078	RpL23	YES	No	Known	No	0.93	-1.01	-1.93	0.06	0.37	0.31
FBgn0010409	RpL18A	YES	No	Known	No	0.48	-0.88	-1.35	0.31	0.57	0.26
FBgn0014026	RpL7A	YES	No	Known	No	0.71	-0.79	-1.51	0.14	0.62	0.48
FBgn0033699	RpS11	YES	No	Known	No	0.26	-1.35	-1.61	0.22	0.84	0.62
FBgn0034138	RpS15	YES	No	Known	No	0.31	-1.04	-1.35	0.25	0.70	0.45
FBgn0039406	RpL34a	YES	No	Known	No	0.39	-1.38	-1.77	-0.44	0.00	0.44
FBgn0000100	RpLP0	YES	No	Known	No	0.62	-1.04	-1.67	0.23	0.82	0.59

FBgn0037270	eIF3f1	No	YES	Known	No	0.73	-0.38	-1.12	0.41	0.59	0.18
FBgn0002590	RpS5a	YES	No	Known	No	0.45	-0.19	-0.63	0.38	0.44	0.06
FBgn0003279	RpL4	YES	No	Known	No	1.01	-0.97	-1.98	0.34	0.41	0.07
FBgn0004403	RpS14a	YES	No	Known	No	0.70	-1.27	-1.97	0.40	1.31	0.91
FBgn0004404	RpS14b	YES	No	Known	No	0.57	-1.22	-1.79	0.42	1.26	0.84
FBgn0005593	RpL7	YES	No	Known	No	0.48	-0.77	-1.25	0.11	1.11	1.00
FBgn0010198	RpS15Aa	YES	No	Known	No	0.03	-1.75	-1.78	0.46	1.27	0.81
FBgn0010412	RpS19a	YES	No	Known	No	0.64	-1.27	-1.90	0.35	0.44	0.09
FBgn0015521	RpS21	YES	No	Known	No	0.96	-1.12	-2.08	0.21	0.71	0.50
FBgn0015756	RpL9	YES	No	Known	No	0.10	-0.55	-0.65	0.51	0.67	0.17
FBgn0017545	RpS3A	YES	No	Known	No	-0.20	-1.54	-1.34	0.56	0.92	0.36
FBgn0019936	RpS20	YES	No	Known	No	0.22	-0.84	-1.07	0.18	0.71	0.53
FBgn0023170	RpL39	YES	No	Known	No	-0.12	-1.77	-1.65	0.60	1.21	0.60
FBgn0030616	RpL37a	YES	No	Known	No	1.00	-1.57	-2.57	0.16	0.59	0.43
FBgn0032518	RpL24	YES	No	Known	No	0.87	-0.38	-1.25	0.48	0.64	0.16
FBgn0032987	RpL21	YES	No	Known	No	0.02	-2.07	-2.09	0.15	1.06	0.91
FBgn0033555	RpS15Ab	YES	No	Known	No	-0.02	-0.15	-0.13	0.23	-0.07	-0.31
FBgn0034968	RpL12	YES	No	Known	No	0.45	-0.77	-1.22	0.16	0.78	0.62
FBgn0035753	RpL18	YES	No	Known	No	1.08	-0.92	-2.00	0.54	0.75	0.22
FBgn0036213	RpL10Ab	YES	No	Known	No	0.33	-1.12	-1.44	0.31	0.64	0.33
FBgn0037686	RpL34b	YES	No	Known	No	1.22	-0.47	-1.69	0.22	0.20	-0.02
FBgn0039129	RpS19b	YES	No	Known	No	0.11	-1.35	-1.45	-0.82	-0.65	0.18
FBgn0040007	RpL38	YES	No	Known	No	-0.12	-1.55	-1.43	0.91	1.13	0.22
FBgn0064225	RpL5	YES	No	Known	No	0.06	-1.28	-1.34	0.83	1.17	0.34
FBgn0086472	RpS25	YES	No	Known	No	0.36	-0.71	-1.07	-0.06	0.53	0.59
FBgn0086710	RpL30	YES	No	Known	No	0.58	-1.20	-1.78	0.07	1.05	0.98
FBgn0261593	RpS10b	YES	No	Known	No	0.96	-1.20	-2.16	0.57	0.94	0.36
FBgn0261597	RpS26	YES	No	Known	No	0.86	-1.29	-2.15	0.93	0.93	0.00
FBgn0002593	RpLP1	YES	No	Known	No	0.67	-0.44	-1.12	0.39	0.72	0.34
FBgn0003274	RpLP2	YES	No	Known	No	0.64	-1.26	-1.90	0.23	0.50	0.27
FBgn0001215	Hrb98DE	No	No	Known	No	-0.50	-0.73	-0.23	0.14	0.25	0.11
FBgn0004237	Hrb87F	No	No	Known	No	-0.07	-0.36	-0.29	0.19	0.15	-0.04
FBgn0037874	Tctp	No	No	Known	No	0.05	-1.30	-1.36	0.21	0.54	0.33
FBgn0050185	CG30185	No	No	Known	No	0.18	-0.52	-0.70	0.03	-0.27	-0.30
FBgn0265297	pAbp	No	No	Known	No	-0.02	-0.39	-0.38	0.64	1.04	0.40
FBgn0028737	Ef1beta	No	YES	Known	No	0.64	-0.93	-1.57	0.28	0.45	0.17
FBgn0029176	Ef1gamma	No	YES	Known	No	0.66	-0.89	-1.55	0.16	0.62	0.46
FBgn0032198	eEF1delta	No	YES	Known	No	-1.06	-0.96	0.10	-0.16	-0.34	-0.18
FBgn0011272	RpL13	YES	No	Novel	No	0.75	-1.11	-1.86	0.42	0.29	-0.14
FBgn0039790	CG2246	No	No	Novel	No	0.34	-0.18	-0.53	0.11	0.27	0.15
FBgn0020910	RpL3	YES	No	Novel	No	0.62	0.02	-0.60	0.37	0.77	0.40
FBgn0028697	RpL15	YES	No	Novel	No	0.09	-2.14	-2.23	0.56	1.30	0.74
FBgn0032404	RpL7-like	YES	No	Novel	No	0.21	-1.37	-1.58	0.10	0.36	0.26

FBgn0034361	mRpS28	YES	No	Novel	No	0.42	-0.74	-1.16	-0.01	0.36	0.38
FBgn0039300	RpS27	YES	No	Novel	No	0.81	-0.12	-0.92	-0.20	0.01	0.21
FBgn0039359	RpL27	YES	No	Novel	No	0.40	-1.73	-2.13	0.24	1.06	0.82
FBgn0039713	RpS8	YES	No	Novel	No	0.98	-0.51	-1.49	0.32	0.58	0.26
FBgn0261599	RpS29	YES	No	Novel	No	0.39	-0.16	-0.54	0.28	1.07	0.78
FBgn0261606	RpL27A	YES	No	Novel	No	0.51	-0.78	-1.30	0.20	0.29	0.09
FBgn0000826	png	No	No	Novel	No	1.04	-0.06	-1.10	-0.32	-0.34	-0.03
FBgn0001091	Gapdh1	No	No	Novel	No	0.21	-0.66	-0.87	-0.11	-0.08	0.02
FBgn0010417	Taf6	No	No	Novel	No	0.85	0.13	-0.71	-0.06	0.25	0.31
FBgn0010602	lwr	No	No	Novel	No	0.50	-0.12	-0.61	-0.38	-0.33	0.05
FBgn0010808	l(3)03670	No	No	Novel	No	0.36	-0.67	-1.04	-0.22	0.00	0.23
FBgn0011768	Fdh	No	No	Novel	No	0.22	-0.88	-1.10	-0.14	-0.07	0.07
FBgn0015019	Cctgamma	No	No	Novel	No	-0.19	-1.01	-0.82	-0.09	-0.02	0.07
FBgn0021979	l(2)k09913	No	No	Novel	No	0.93	0.30	-0.62	0.18	0.26	0.08
FBgn0025814	Mgstl	No	No	Novel	No	0.09	-0.62	-0.71	0.00	-0.59	-0.59
FBgn0026409	Mpcp	No	No	Novel	No	0.39	-0.51	-0.89	0.25	0.38	0.13
FBgn0027080	Aats-tyr	No	No	Novel	No	0.30	-0.73	-1.03	-0.27	0.12	0.39
FBgn0027335	Rip11	No	No	Novel	No	0.70	0.18	-0.52	-0.22	-0.41	-0.19
FBgn0027525	CG7686	No	No	Novel	No	0.79	0.01	-0.78	0.19	0.66	0.48
FBgn0029830	Grip	No	No	Novel	No	0.63	0.08	-0.56	0.23	0.14	-0.09
FBgn0030151	CG1354	No	No	Novel	No	0.20	-0.80	-1.01	-0.45	0.05	0.50
FBgn0031053	CG14223	No	No	Novel	No	1.26	0.05	-1.22	-0.29	-0.22	0.07
FBgn0031450	Hrs	No	No	Novel	No	0.81	0.27	-0.54	-0.12	-0.11	0.01
FBgn0031664	CG8892	No	No	Novel	No	0.33	-0.24	-0.58	-0.18	-0.45	-0.28
FBgn0032089	Rcd-1r	No	No	Novel	No	-0.30	-1.00	-0.70	-1.27	-1.13	0.15
FBgn0035445	CG12014	No	No	Novel	No	0.63	-0.17	-0.81	-0.39	-0.21	0.19
FBgn0036877	CG9452	No	No	Novel	No	0.51	0.01	-0.50	-1.48	-1.18	0.30
FBgn0036974	eRF1	No	No	Novel	No	-0.20	-0.95	-0.75	0.36	0.40	0.04
FBgn0037688	CG9356	No	No	Novel	No	0.49	-0.15	-0.64	-0.46	0.10	0.56
FBgn0039337	MED28	No	No	Novel	No	0.34	-0.36	-0.69	-0.31	-0.59	-0.29
FBgn0039881	CG1971	No	No	Novel	No	0.23	-0.39	-0.62	-0.96	-0.74	0.22
FBgn0086904	Nacalpha	No	No	Novel	No	0.55	-0.85	-1.39	0.32	0.52	0.19
FBgn0015834	Trip1	No	YES	Novel	No	0.06	-0.70	-0.77	0.14	0.44	0.30

Source: known, homologous to known 5' TOP gene in human; novel, this study.
tsRNA Target: strong targets of tsRNAs in S2 cell

Table S7 Predicted target genes of the nine tsRNAs that are involved in the global translational regulation

tsRNA	gene ID	gene name
T3	FBgn0029095	aru
T3	FBgn0037529	mRpS9
T3	FBgn0053158	CG33158
T6	FBgn0020443	Elf
T10	FBgn0053155	CG33155
T10	FBgn0053158	CG33158
T10	FBgn0066084	RpL41
T10	FBgn0086706	pix
T13	FBgn0000556	Ef1alpha48D
T13	FBgn0000559	EF2
T13	FBgn0002593	RpLP1
T13	FBgn0005533	RpS17
T13	FBgn0010408	RpS9
T13	FBgn0013325	RpL11
T13	FBgn0015288	RpL22
T13	FBgn0027087	Aats-his
T13	FBgn0028744	CG5033
T13	FBgn0032138	CG4364
T13	FBgn0033912	RpS23
T13	FBgn0034087	clu
T13	FBgn0034743	RpS16
T13	FBgn0036774	mRpS26
T13	FBgn0039175	CG5706
T13	FBgn0039182	CG5728
T13	FBgn0040227	eIF-3p66
T13	FBgn0261602	RpL8
T14	FBgn0000559	EF2
T14	FBgn0003942	RpS27A
T14	FBgn0004407	DNApol-gamma35
T14	FBgn0011284	RpS4
T14	FBgn0024556	EfTuM
T14	FBgn0029176	Ef1gamma
T14	FBgn0034087	clu
T14	FBgn0034858	eIF2B-delta
T14	FBgn0036686	CG7728
T14	FBgn0036974	eRF1
T14	FBgn0037270	CG9769
T14	FBgn0038834	RpS30
T14	FBgn0053155	CG33155
T14	FBgn0066084	RpL41
T14	FBgn0086706	pix
T15	FBgn0000556	Ef1alpha48D
T15	FBgn0000559	EF2
T15	FBgn0001942	eIF-4a
T15	FBgn0004407	DNApol-gamma35
T15	FBgn0005674	Aats-glupro
T15	FBgn0010078	RpL23
T15	FBgn0011272	RpL13
T15	FBgn0011284	RpS4
T15	FBgn0015075	Ddx1
T15	FBgn0015806	S6k
T15	FBgn0020305	dbe

T15	FBgn0020443	Elf
T15	FBgn0022023	eIF-3p40
T15	FBgn0024182	waw
T15	FBgn0024251	bbx
T15	FBgn0026196	nop5
T15	FBgn0026259	eIF5B
T15	FBgn0028744	CG5033
T15	FBgn0028962	Aats-ala-m
T15	FBgn0030063	CG1789
T15	FBgn0032050	CG13096
T15	FBgn0032138	CG4364
T15	FBgn0032298	CG6724
T15	FBgn0032404	RpL7-like
T15	FBgn0032486	CG5705
T15	FBgn0033379	Mys45A
T15	FBgn0034029	eIF2B-gamma
T15	FBgn0034401	CG15100
T15	FBgn0034743	RpS16
T15	FBgn0035064	Aats-tyr-m
T15	FBgn0037249	eIF3-S10
T15	FBgn0038146	CG9799
T15	FBgn0039406	RpL34a
T15	FBgn0039588	CG12413
T15	FBgn0039757	RpS7
T15	FBgn0039857	RpL6
T15	FBgn0040227	eIF-3p66
T15	FBgn0053158	CG33158
T15	FBgn0083983	mRpL34
T15	FBgn0086706	pix
T15	FBgn0261593	RpS10b
T15	FBgn0261602	RpL8
T16	FBgn0003517	sta
T16	FBgn0010408	RpS9
T16	FBgn0017579	RpL14
T16	FBgn0020305	dbe
T16	FBgn0024182	waw
T16	FBgn0024251	bbx
T16	FBgn0027084	Aats-lys
T16	FBgn0027087	Aats-his
T16	FBgn0029176	Ef1gamma
T16	FBgn0032050	CG13096
T16	FBgn0033741	CG8545
T16	FBgn0034858	eIF2B-delta
T16	FBgn0035942	CG5660
T16	FBgn0036569	CG5414
T16	FBgn0036686	CG7728
T16	FBgn0036974	eRF1
T16	FBgn0037073	CG7338
T16	FBgn0037270	CG9769
T16	FBgn0038834	RpS30
T16	FBgn0039359	RpL27
T16	FBgn0039555	mRpS22
T16	FBgn0039566	CG4849
T16	FBgn0039588	CG12413
T16	FBgn0051133	Slimp
T16	FBgn0053155	CG33155
T16	FBgn0260441	RpS12
T16	FBgn0261602	RpL8

T17	FBgn0000100	RpLP0
T17	FBgn0000559	EF2
T17	FBgn0002607	RpL19
T17	FBgn0002622	RpS3
T17	FBgn0002626	RpL32
T17	FBgn0005674	Aats-glupro
T17	FBgn0010409	RpL18A
T17	FBgn0010803	Aats-trp
T17	FBgn0011272	RpL13
T17	FBgn0011284	RpS4
T17	FBgn0014026	RpL7A
T17	FBgn0015806	S6k
T17	FBgn0019949	Cdk9
T17	FBgn0021995	Rs1
T17	FBgn0023512	eIF2B-epsilon
T17	FBgn0025582	Int6
T17	FBgn0026372	RpL23A
T17	FBgn0027079	Aats-val
T17	FBgn0027084	Aats-lys
T17	FBgn0027087	Aats-his
T17	FBgn0029664	CG10802
T17	FBgn0029785	RpL35
T17	FBgn0030007	CG2263
T17	FBgn0030786	mRpL22
T17	FBgn0031980	RpL36A
T17	FBgn0032404	RpL7-like
T17	FBgn0033379	Mys45A
T17	FBgn0033741	CG8545
T17	FBgn0033912	RpS23
T17	FBgn0034087	clu
T17	FBgn0034401	CG15100
T17	FBgn0034858	eIF2B-delta
T17	FBgn0036135	mRpL2
T17	FBgn0036629	CG4573
T17	FBgn0037073	CG7338
T17	FBgn0038834	RpS30
T17	FBgn0038923	mRpL35
T17	FBgn0039182	CG5728
T17	FBgn0039828	CG1542
T17	FBgn0040389	mRpL14
T17	FBgn0051739	CG31739
T17	FBgn0053123	CG33123
T17	FBgn0086706	pix
T17	FBgn0260460	mRpS34
T17	FBgn0261593	RpS10b
T17	FBgn0261597	RpS26
T17	FBgn0261602	RpL8
T18	FBgn0000559	EF2
T18	FBgn0002593	RpLP1
T18	FBgn0010409	RpL18A
T18	FBgn0011272	RpL13
T18	FBgn0015756	RpL9
T18	FBgn0020305	dbe
T18	FBgn0027079	Aats-val
T18	FBgn0027085	Aats-leu
T18	FBgn0029176	Ef1gamma
T18	FBgn0030007	CG2263
T18	FBgn0031639	mRpS2

T18	FBgn0033548	CG7637
T18	FBgn0033699	RpS11
T18	FBgn0037249	eIF3-S10
T18	FBgn0037529	mRpS9
T18	FBgn0038146	CG9799
T18	FBgn0039153	CG5463
T18	FBgn0039566	CG4849
T18	FBgn0051739	CG31739
T18	FBgn0066084	RpL41

Table S8. The 7-mer motifs whose densities are positively correlated with the *fe* scores in the AGO2 CLIP-Seq data

Sequence of 7-mer	Spearman's correlation with fold changes of RPKM		Differences in densities of this 7-mer between RPs/IEFs and the remaining genes (Among all expressed genes)			Differences in densities of this 7-mer between RPs/IEFs and the remaining genes (Among tsRNA target genes)		
	rho	*P*	RPs/IEFs (mean)	Remaining genes (mean)	*P*	RPs/IEFs (mean)	Remaining genes (mean)	*P*
AAGAAGG	0.573	4.7E-10	1.847	0.268	4.4E-13	2.337	0.368	7.9E-10
CAAGAAG	0.613	1.2E-11	3.141	0.424	3.4E-24	4.256	0.579	5.0E-16
CAAGACC	0.435	6.2E-06	0.891	0.145	5.5E-08	0.974	0.195	1.5E-04
CCAAGAA	0.484	3.5E-07	1.700	0.264	4.7E-15	2.117	0.330	6.2E-11
CCGCAAG	0.493	1.9E-07	1.017	0.138	2.1E-06	1.336	0.174	1.3E-04
CGCAAGG	0.445	3.5E-06	0.981	0.164	3.7E-05	1.483	0.211	1.9E-06
GAAGAAG	0.363	2.0E-04	1.957	0.318	4.6E-10	2.785	0.381	3.9E-13
GCAAGGT	0.496	1.6E-07	0.767	0.100	1.3E-05	0.810	0.120	1.5E-04

In the Spearman's correlation analysis, for each motif, the genes were grouped into 100 bins based on increasing densities of the 7-mer motif and the correlation was calculated between the mean density of that motif and the mean *fe* score in each bin.